Reprinted from Journal of the Optical Society of America A, Vol. 2, p. 267, February 1985
Copyright © 1985 by the Optical Society of America and reprinted by permission of the copyright owner.

Detection and discrimination of sinusoidal grating displacements

Ken Nakayama and Gerald H. Silverman

Smith-Kettlewell Institute of Visual Sciences, Medical Research Institute of San Francisco, 2200 Webster Street, San Francisco, California 94115

Received June 5, 1984; accepted October 2, 1984

Vertical sine-wave gratings of varying spatial frequency were stepped instantaneously to the right or to the left at differing phase angles (θ). Separate paradigms measured the contrast threshold for the *detection* of such a step and for the *discrimination* of the direction of the same step. By considering the grating before and after its displacement as a rotating phasor, we made the following predictions: (1) Contrast sensitivity for the detection of a displacement should rise as $\sin(\theta/2)$. (2) Contrast sensitivity for the discrimination of the direction of the displacement should rise as $\sin(\theta)$. Both predictions were confirmed using a range of spatial frequencies and phase angles. From the results of additional experiments, by measuring the discrimination of the direction thresholds as a function of contrast, we derived a nonlinear contrast response function for the motion system. This function appears to saturate fully at fairly low levels, in the neighborhood of 2 to 3% under the conditions examined. Our results suggest a direct connection among the contrast sensitivity, the contrast response function, and motion-hyperacuity thresholds.

INTRODUCTION

Many experiments designed to probe the nature of motion sensitivity have used discontinuous step(s) of random dots.[1–6] For a given target configuration of these dots, there is a maximum as well as a minimum stimulus displacement that can be seen as moving coherently. The maximum limit has also been considered in terms of the spatial-frequency content of the moving stimulus or equivalently in terms of the size of the input receptive fields (RF's) hypothesized to mediate motion sensitivity. In particular, it has been suggested that motion-sensitive systems fed by large RF's can encode coherent motion in random dots over longer distances than those fed by smaller RF's.[4,5]

In this paper, we explore this issue of RF size by using sinusoidal gratings because these gratings have the property of restricting the excitation to the smallest range of RF sizes. Sinusoidal gratings have been used extensively as a method to probe motion sensitivity but, rather than stepping the gratings, previous investigators have drifted the gratings continuously. Some investigators have measured the contrast sensitivity to sense direction,[7] and others have measured the sensitivity to generate direction-specific adaptation.[8] In this paper, we fill a needed experimental gap by displacing sinusoidal gratings by a variable phase angle and by measuring contrast sensitivity either to see the presence of motion or to discriminate its direction.

METHOD

Vertical sinusoidal gratings were generated on a cathode-ray oscilloscope monitor (HP 1332A) by using conventional television techniques. Luminance was 12 cd/m^2. Linearity of contrast modulation was maintained to within 2% up to a maximum Michelson contrast of 32%. Contrast = $(L_{max} - L_{min})/(L_{max} + L_{min})$. Photometric measurements were made by a Pritchard Spectra spot meter. Unless specified, the viewing distance was 114 cm and the square display subtended an angle of 5° × 5°. The subject viewed a fixation point at the center of the screen.

Detection Thresholds

In this experiment, we fixed the phase-angle jump size (θ) and measured the contrast sensitivity. We used a two-alternative forced-choice procedure in which the grating appeared twice in succession, separated by the 1.5-sec interval. In just one of these intervals, the grating underwent an instantaneous phase-angle jump, whose magnitude was fixed for a particular run. In the other interval, there was no displacement. In practice, the jump has a nominal duration of 10 msec because the frame rate of the cathode-ray tube (CRT) was 100 Hz. Hardware timing signals ensured that the phase jump always occurred during the CRT raster-retrace period, eliminating any displacement-onset artifact. The observer's task was to identify the temporal interval in which the displacement occurred. To reduce the uncertainty about the exact temporal position of the two intervals, the middle of each interval was accompanied by an audible click from a loudspeaker. Figure 1A summarizes this two-alternative forced-choice procedure.

Discrimination Thresholds

To measure the contrast sensitivity of the displacement discrimination, we used a one-interval forced-choice technique. The observer was presented with a single interval defined by the presentation of a grating. Halfway during the appearance of the grating, this grating shifted either to the right or to the left on a random basis, and the observer's task was to identify the direction of the shift. In all other respects, the experimental apparatus was the same as that used for detection as described above (see Figure 1B).

0740-3232/85/020267-08$02.00 © 1985 Optical Society of America

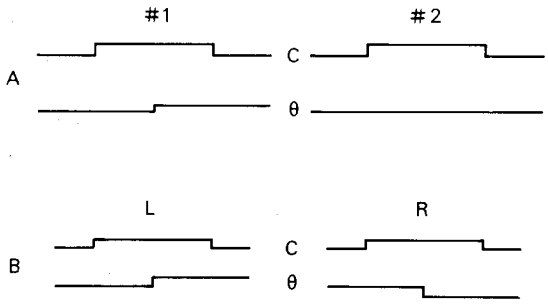

Fig. 1. A, Two-alternative forced-choice paradigm to obtain detection of displacement thresholds. A sinusoidal grating appears twice, defining two temporal intervals. During only one of the inverals is there a phase shift in either direction, denoted by the step in the phase trace (θ). The observer's only task is to identify the time interval (either #1 or #2) containing the phase shift. B, One-alternative forced-choice paradigm to obtain discrimination thresholds. The observer sees one of two possibilities presented at random. The target grating steps either to the right as in R or to the left as in L. The observer's task is to identify the direction of motion.

GENERAL PROCEDURE

We used the psychophysical method of constant stimuli. In the majority of the experiments, we fixed the phase-angle jump (θ) and presented the observer with an array of five contrast levels. We call this the $C = F(\theta)$ experiment. Under some circumstances (see Experiment 4, below), however, it was more practical to do the reverse, i.e., to keep the contrast fixed for a given experimental run and then to present the observer with a distribution of five phase angles. We call this the $\theta = F(C)$ experiment.

To calculate thresholds, we used a probit analysis, fitting the maximum-likelihood estimate of a cumulative Gaussian from the percent-correct distributions.[9] From this we obtained a contrast threshold or a phase-angle threshold that was 75% correct. Each raw threshold value plotted in this paper was determined on the basis of at least 400 and often 800 trials.

It should be noted that the starting phase angle for all experimental trials was randomized from trial to trial, with a range of 128 starting phases being equally probable.

THEORY

Here, we develop our theoretical predictions for each experimental paradigm.[10] To outline our predictions, we present the amplitude and the position of the sine-wave grating in terms of the orthogonal sine and cosine components, thereby plotting the sine wave in a polar or phasor form. Thus the grating is represented by an arrow with its tail at the origin. The contrast of a sinusoidal grating is denoted by the arrow length. Its change in position is denoted by a phase angle (θ). The initial appearance of the grating is defined to be in the cosine phase and lies along the X axis.

Jumping a sine-wave grating can be represented by a step rotation of the arrow through an angle θ. This can be seen in Fig. 2, where the initial grating (described by the vector $\mathbf{G}_i$) has been stepped three eighths of a cycle to its final position represented by $\mathbf{G}_f$. Thus the displacement can be represented by a phase angle (θ), which is equal to 135° in this illustration. Our initial predictions are based on the assumption that the excitation to the visual system is proportional to a linear distance in this phasor representation.

First, we consider the case in which an observer is asked to detect the simple presence of a displacement (not its direction). The initial grating is represented by $\mathbf{G}_i$, and the final grating is represented by $\mathbf{G}_f$ (see Fig. 2A). A simple hypothesis is that detection excitation and thus contrast sensitivity should be proportional to length of the difference vector ($\mathbf{S}$) between $\mathbf{G}_i$ and $\mathbf{G}_f$. The magnitude of $\mathbf{S}$ can be represented by the Pythagorean formula for distance

$$|\mathbf{S}| = (\Delta x^2 + \Delta y^2)^{0.5}, \quad (1)$$

where Δx and Δy represent the difference in the cosine and sine components of the two vectors, respectively. It is most useful for our purposes to express the detection excitation as an explicit function of the phase angle. In Appendix A, we derive the following relation:

$$|\mathbf{S}| = 2A \sin(\theta/2), \quad (2)$$

where A is the magnitude of $\mathbf{G}_i$. An obvious consequence of Eq. (2) is that, for detection, sensitivity will rise with the increasing phase angle, with a maximum at 180°.

Now we consider the second case, in which the observer is asked to discriminate the direction of motion. As opposed to detection in which the predicted sensitivity was maximum at 180°, it should be clear that such a 180° displacement carries no information on the direction of motion. It is completely ambiguous since motion in either direction could have

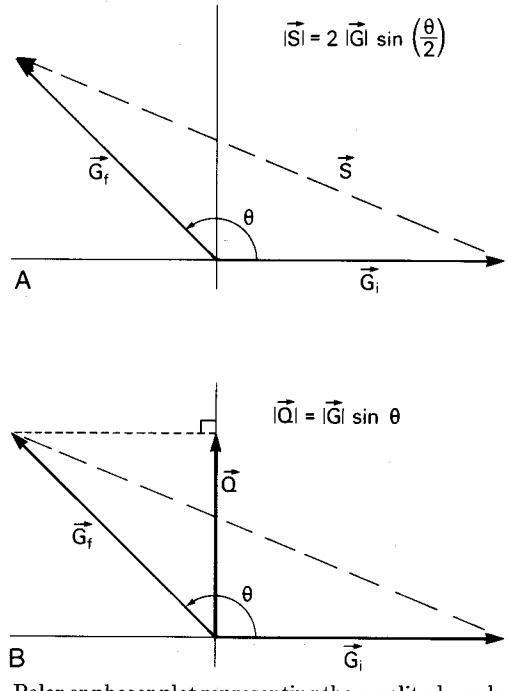

Fig. 2. Polar or phasor plot representing the amplitude and position of a sinusoidal grating before and after a step displacement. $\mathbf{G}_i$ represents the initial grating, arbitrarily defined to be in cosine phase. $\mathbf{G}_f$ represents the final grating after it has been jumped by 135° and when it is in its second position. In A, we describe the hypothetical excitation that can be used to *detect* the existence of step displacement, it being the vector difference between $\mathbf{G}_i$ and $\mathbf{G}_f$. In terms of the phase angle jumped, the excitation is proportional to the sine of one half of the angle (see inset equation in A). In B, we show the hypothetical excitation onto a motion-discrimination system. In this case, it is proportional to the projections of $\mathbf{G}_f$ onto the sine or y axis, which is labeled by the vector $\mathbf{Q}$.

led to the final position. More generally, any component of the difference vector **S** that projects onto the x or cosine axis will carry no directional information (see Fig. 2B). It is only the projection of **S** onto the sine or Y axis that carries directional information. Since the projection of **S** onto this axis is the same as the projection of $\mathbf{G}_f$ onto this axis, it should be clear that the hypothetical excitation or sensitivity for discrimination as a function of phase angle will be different from that of detection. By inspection, it is a simple sine function of θ:

$$\text{Discrimination sensitivity} = ABS\,|A\,\sin(\theta)|. \qquad (3)$$

Therefore the theoretical discrimination sensitivity will be maximum for $\theta = 90°$ and not for $\theta = 180°$, as is the case for simple detection.

RESULTS

Experiment 1: Effect of Grating Duration

Before describing the main experiments, it is important to establish whether the duration of the grating is critical and to pick an appropriate duration if it is. On the one hand, we wanted to make the grating duration long enough so the response to the grating onset reached some reasonable steady-state value before the grating moved to its new position. On the other hand, we did not want to make the grating appearance too long, lest we activate some form of adaptation to contrast.[11,12] To address this issue, we varied the duration of the grating over an eightfold range (from 50 to 400 msec) and measured contrast sensitivity to discriminate motion when the phase-angle jump was 90°. Figure 3 shows that over a significant range of duration there is only a small change in contrast sensitivity. As there was a shallow but discernable peak for the 200-msec duration, we chose this for the experiments reported herein.

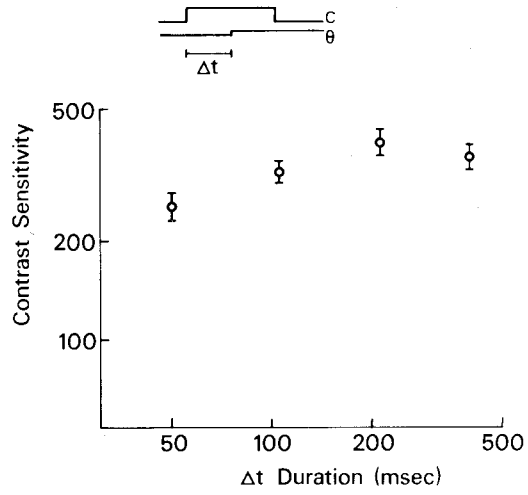

Fig. 3. Effect of grating duration Δt (see inset) on contrast sensitivity for experiments in which the observer was required to discriminate direction. Phase shift is 90°. Spatial frequency is 2 cyc/deg. The subject is KN.

Experiment 2: Detection of Grating Displacement

Our hypothetical model predicts that contrast sensitivity for detection should rise as the sine of half of the angle jumped as in Eq. (2). In Fig. 4A, we plot raw contrast sensitivity (the reciprocal of contrast threshold) as a function of the phase angle for stepped gratings of 2 and 8 cycles/degree (cyc/deg). The quarter sinusoidal wave form shown is the best least-squares fit to the data, conforming to $K\,\sin(\theta/2)$, where K is the constant to be fitted. Figure 4B shows the results of these two spatial frequencies, normalized and averaged. It should be clear that the fit of the data with respect to our theoretical prediction is excellent, showing a maximum contrast sensitivity for 180° phase shifts.

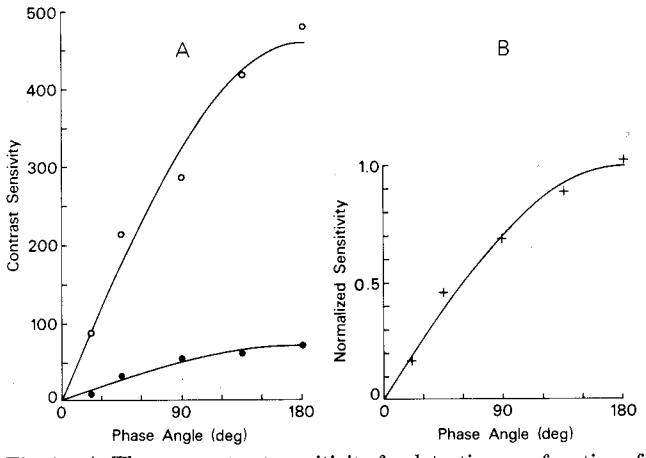

Fig. 4. A, The raw contrast sensitivity for detection as a function of the phase angle for 2 and 8 cyc/deg. B, Contrast sensitivity of the best-fitting theoretical curve has been normalized to one, and both sets of data have been averaged. Note the linear scale for contrast sensitivity. The subject is JS.

Experiment 3: Contrast Sensitivity as a Function of Phase Angle for Discrimination

It should be remembered that our theoretical predictions for the discrimination of motion were quite different from those for detection, conforming to a simple sine function of the phase angle. The results of a number of discrimination experiments can be seen in Fig. 5A, which shows the raw (non-normalized) contrast sensitivities as a function of the phase angle for three spatial frequencies (2, 4, 8 cyc/deg). Figure 5B shows the normalized and the averaged contrast sensitivities for these and one additional spatial frequency (1, 2, 4, 8

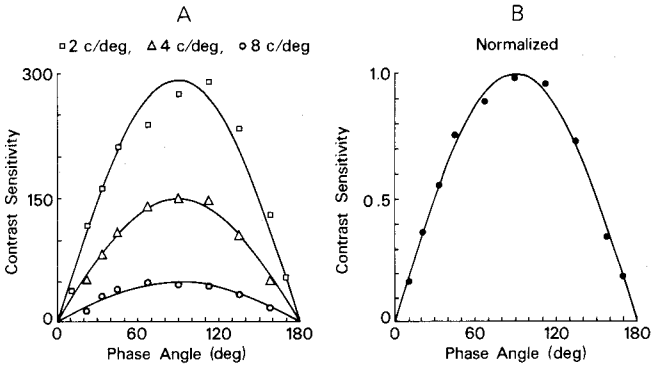

Fig. 5. Contrast sensitivity for the discrimination of motion direction. A, Raw contrast sensitivities as a function of phase angle for 2 cyc/deg (squares), 4 cyc/deg (triangles), and 8 cyc/deg (circles). B, Normalized and averaged contrast sensitivity for 1, 2, 4, 8 cyc/deg. Note linear scale for contrast sensitivity. The subject is JS.

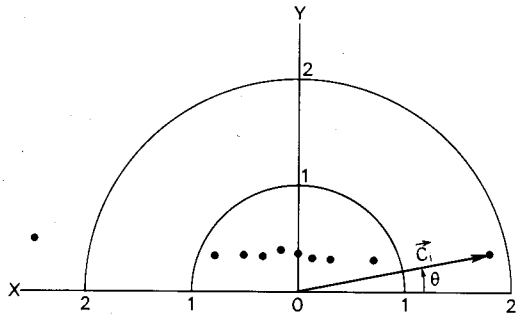

Fig. 6. Polar coordinate representation of discrimination contrast thresholds taken from Fig. 5A (2 cyc/deg). Distance of the data point from the origin defines a radius vector whose length is proportional to the contrast of the grating and whose angle with respect to the positive X axis defines the phase angle jumped. The radius vector $\mathbf{C}_i$ and phase angle θ_i are illustrated for just one data point by the arrow. Semicircles represent grating contrasts of 1 and 2%, respectively. Note that, with the possible exception of the leftmost point, all data fall on a horizontal line, which by definition has the same projection onto the y axis.

cyc/deg). The discrimination results fit the simple sine-wave prediction surprisingly well, showing the expected peak at 90°.

So far, we have plotted our results in terms of contrast sensitivity versus phase angle in order to illustrate how the data of both the detection and the discrimination experiments conformed to the experimental predictions, as outlined by Eqs. (2) and (3). To illustrate a different way to view the discrimination results, we plot contrast thresholds for displacement discrimination linearly in phasor coordinates, as originally represented in Fig. 2. For example, in Fig. 6, we take the 2-cyc/deg data from Fig. 5A and plot the phase angle jumped as an angle θ with respect to the positive X axis and plot the contrast threshold of the grating as a distance from the origin. From this graph, it should be clear that for a phase angle of 90° the contrast is the lowest, which is a result equivalent to the peak sensitivity seen for 90° shifts in Fig. 5. For greater and greater deviations from 90°, the contrast required for the discrimination becomes progressively increased. An advantage of this vector representation is that it nicely illustrates the essentially identical linear projection of each of these rather different magnitude-contrast vectors onto the Y axis. As such, we can provide a simple linear rule as to whether the direction of a given grating displacement will be discriminated. If its linear projection onto the Y axis exceeds the threshold obtained for a 90° phase shift, it can be discriminated. Since we will use this 90° threshold to draw further conclusions, we define it as the quadrature threshold, T_Q.

MEASUREMENT OF THE MINIMUM-MOTION THRESHOLD (D_{min})

At this point, we relate our present results to motion thresholds obtained using more complex stimuli including random dot patterns. In particular, we focus on D_{min}, the minimum amount of motion that can be perceived, also called the motion hyperacuity threshold.[13] Under the most favorable conditions, the motion-hyperacuity threshold is about 5 arc sec.[14] In other studies, which use displaced sine waves, a somewhat higher threshold has been obtained, about 10 arc sec.[15] The threshold value of D_{min} is roughly comparable with those of the thresholds obtained for static hyperacuity tasks, such as vernier acuity.

Here, we discuss some implications of our direction-discrimination function to make predictions regarding motion-hyperacuity thresholds. Our theoretical argument has two stages. First, we assume linearity and show it to be untenable for high-contrast gratings. Then we develop an approach to characterize the nonlinearity.

We start by assuming that our model relating the phase angle to the contrast sensitivity (Fig. 2B) can be linearly extrapolated to predict phase-angle thresholds for any given contrast. One can pick a contrast ($\mathbf{C}_i$), and the corresponding phase-angle displacement (ϕ) associated with that contrast can be derived by calculating the angle for which the projection of the input contrast vector $\mathbf{C}_i$ is equal to T_Q (see Fig. 7):

$$\phi = \arcsin(T_Q/\mathbf{C}_i), \tag{4}$$

where ϕ is the predicted phase angle of the jump, T_Q is the quadrature threshold, and $\mathbf{C}_i$ is the input contrast vector. Clearly the model works for the data presented so far, because it conforms to the sine function in Fig. 5 and to the straight line representing the same data plotted in polar form (Fig. 6).

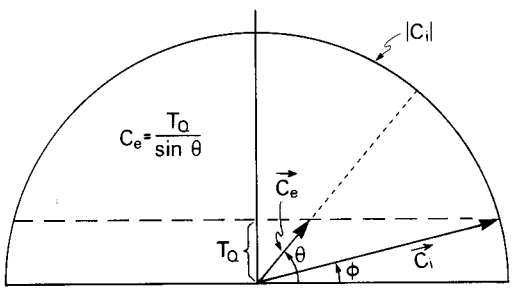

Fig. 7. Derivation of the effective contrast for motion discrimination. We assume that motion discrimination requires a minimum amount of energy to be projected onto the orthogonal or quadrature axis (T_Q). If the coding of effective contrast were linear, then given any input contrast $\mathbf{C}_i$ we can predict the displacement threshold (ϕ) [see Eq. (4)]. This can be seen by noting arrow $\mathbf{C}_i$ and its associated phase angle (ϕ). If the system had a compressive nonlinearity, then the effective contrast $\mathbf{C}_e$ would be smaller than $\mathbf{C}_i$. For $\mathbf{C}_e$ to project equally on to the Y axis with a value of T_Q, θ would have to be correspondingly larger. As such, a measurement of θ also permits an estimate of $\mathbf{C}_e$. See the equation in the inset, which is the same as Eq. (5). Note that the angles in this figure are not drawn to scale; they have been increased for purposes of clarity.

As yet, however, we have presented only data of gratings having relatively low contrast. The question to be asked is whether one can use Eq. (4) to predict the displacement threshold for any contrast, including the highest contrasts possible. Since the grating can reach a maximum contrast value of 100%, we can predict the minimum displacement thresholds for a sinusoidal grating of a given spatial frequency by substituting unity for $\mathbf{C}_i$ in Eq. (4). Using the contrast threshold at 90° for subjects KN and JS at 2 cyc/deg, we obtain predicted phase-angle thresholds of 0.12 and 0.2 deg. Because the grating has a spatial frequency of 2 cyc/deg, these phase-angle thresholds correspond to displacement thresholds of 0.6 and 1.0 arc sec, respectively. It should be apparent that these values for a predicted motion-hyperacuity threshold are very low, being almost an order of magnitude lower than the best threshold of 5 arc sec that has been reported for motion.[14]

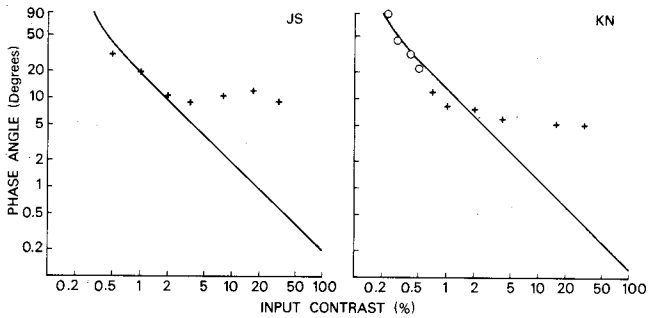

Fig. 8. Phase-angle thresholds as a function of grating contrast. Crosses are data from the $\theta = F(c)$ experiment. Circles are data from the $\mathbf{C} = F(\theta)$ experiment. The spatial frequency is 2 cyc/deg. The solid line is the best-fitting sinusoid to account for contrast thresholds in the $\mathbf{C} = F(\theta)$ experiment (as in Fig. 5).

As such, these values indicate the inadequacy of our extrapolated linear model to predict hyperacuity thresholds.

In this section, we explore the alternative of having a hypothetical compressive nonlinearity of the contrast transducer function of the detectors that feed into the motion-analyzing system. Consider the case in which we have a much higher contrast grating than that used so far, say, 100%. If the grating contrast was encoded linearly, then the relationship between the phase angle and the contrast at threshold can be expressed by Eq. (4). Suppose, however, that the effective contrast signal no longer rises linearly with input contrast at this high-contrast level but is compressed as contrast is increased. If this were the case, the compressed or effective contrast vector $\mathbf{C}_e$ would have to be rotated over a much larger phase angle (θ) so that its projection would equal T_Q. By simple trigonometry, it should be clear from Fig. 7 that, given the contrast sensitivity at 90° (T_Q) and a measurement of the phase-angle threshold (θ), it is possible to estimate the effective contrast for any contrast input:

$$\mathbf{C}_e = T_Q/\sin(\theta), \tag{5}$$

where θ is the empirically measured phase-angle displacement threshold for a given contrast input $\mathbf{C}_i$ and $\mathbf{C}_e$ is the effective (or compressed) contrast. In the next experiment, we describe the measurements to obtain this value of effective contrast.

Experiment 4: Discrimination of Minimum Phase Angle for Given Values of Contrast: Derivation of Effective Contrast

In the previous experiments, we fixed a rather large phase-angle displacement and measured the contrast sensitivity. In this experiment we do the reverse, measuring the minimum phase angle as a function of rather high fixed values of contrast and conducting the $\theta = F(c)$ experiment.

The results can be seen by referring to Fig. 8, which plots the threshold phase angle as a function of contrast. What should be clear is that above a value of about 2% contrast there is essentially no reduction in the phase-angle displacement threshold for either observer. This should be compared with the theoretical linear prediction relating phase angle to contrast described in Eq. (4) and plotted as the solid curve in Fig. 8. As mentioned earlier, we hypothesize that the deviation from this theoretical prediction is related to contrast saturation in the motion system, and, by applying Eq. (5) to both the $C = F(\theta)$ and the $\theta = F(C)$ data, we can make an estimate of this saturating contrast function. This can be seen in Fig. 9. Note that the effective contrast appears to rise rather linearly over an approximately eightfold range and then quickly saturates at contrast values of about 2%.

DISCUSSION OF EXPERIMENT 4

The fact that higher contrasts had so little value in improving displacement thresholds was surprising to us. We expected to see evidence of saturation but more on the order of that described for static positional tasks. Watt and Morgan,[16] for example, showed that the positional thresholds were inversely proportional to the square root of the contrast. In the present experiments on motion sensitivity, the saturation is more extreme, indicating that the motion system is disregarding and essentially wasting the additional information in gratings having contrasts above values as low as 2%.

Surprising as the results may seem to us, they have ample precedent in a different paradigm used to study motion. After prolonged viewing of moving adapting targets, the strength of the motion aftereffect (measured by a variety of techniques) appears to rise linearly with adapting contrast, but only over a short range, and then saturates rather quickly at three to four times the contrast threshold.[17–19] All these results indicate that for the motion system there is a rather striking degree of contrast saturation at low-contrast levels.

Here, we discuss our results in relation to other psychophysical research on the encoding of contrast. Numerous studies have investigated the question of the contrast transducer function, usually employing masking paradigms to determine the contrast increment needed to see additional contrast in the presence of a mask. These have been reviewed by Legge.[20] The results of such studies vary in a number of significant details, but one general feature stands out that is different from the present results. The encoding of contrast extends up to 100% in most of these studies, whereas we show it to be severely clipped at contrasts as low as 2%.

How do our results compare with contrast response func-

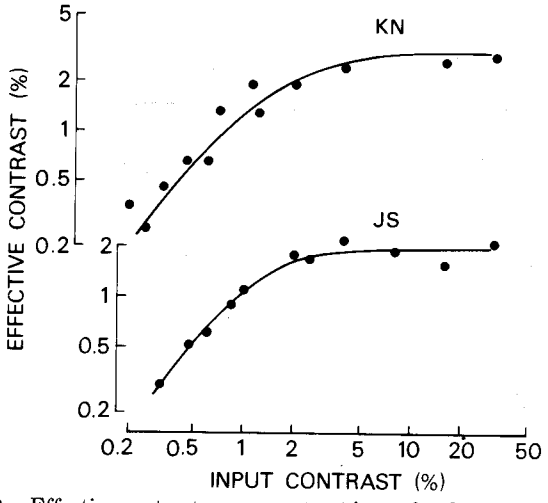

Fig. 9. Effective contrast versus contrast input for the motion system. A shows the effective contrast response output versus input derived from the data of Fig. 5B and of Fig. 9 for observer JS. Derivation is based on Eq. (5). B shows similar data taken from observer KN. All data are taken at 2 cyc/deg. Solid lines represent the best-fitting hyperbolic-ratio functions [see Eq. (6)].

tions obtained electrophysiologically? The most complete study has been conducted by Albrecht and Hamilton,[21] who measured contrast response functions for more than 200 cortical neurons in cat and monkey striate cortex. An overwhelming number of cells were best fitted by a hyperbolic-ratio function, and most of the small remaining population of neurons were fitted, if not optimally, at least rather adequately by the same function. It has the form

$$R = k\mathbf{C}^n/(\mathbf{C}^n + \mathbf{C}_{50}{}^n), \quad (6)$$

where k is the asymptotic output contrast (in percent), $\mathbf{C}$ is the input contrast vector, n is a positive exponent, and $\mathbf{C}_{50}$ is the semisaturation constant (the value of contrast at which the response reaches half maximum). For all units, n had a mean of 2.9 and $\mathbf{C}_{50}$ had a mean of 19.3, but there was widespread variability in each of these parameters from cell to cell. Although the low-contrast portion of the data in Fig. 9 looks essentially linear, it is also statistically indistinguishable from a rather linear-looking portion of a hyperbolic-ratio function, having fitting constants of $n = 1.84$ and $\mathbf{C}_{50} = 0.85$ for subject JS and $n = 1.48$ and $\mathbf{C}_{50} = 1.19$ for subject KN (see Fig. 9). These two hyperbolic-ratio functions account for 93 and 96% of the variance, respectively. Regardless of the exact mathematical form of the results, the early saturation suggests that psychophysical displacement thresholds are mediated by only a small subset of the cortical cells described by Albrecht and Hamilton.[21]

At this point, we should caution that our derived measurement of effective contrast obtained psychophysically is perhaps one additional step removed from the contrast response functions measured physiologically. Psychophysical thresholds are limited by signal-to-noise ratios, but these are rarely measured in physiological experiments.[22–24] What is missing is a systematic and comparative estimate of the intrinsic variability of the neural discharge at different contrast levels. If the noise is simply additive, i.e., a baseline upon which a signal is imposed, then the neurophysiological and the psychophysical results are probably comparable. If, on the other hand, the noise rises with response amplitude, then there could be a discrepancy between the psychophysical effective contrast and the class of results obtained by Albrecht and Hamilton.[21]

GENERAL DISCUSSION

Possible Relation to Neurophysiology

We consider some relationships of the present results to current neurophysiological research.

First, there is the hypothetical contrast response function that we have derived. The insensitivity to contrast above a low saturating value was noted early in the characterization of directionally selective neurons. Barlow and Hill,[25] for example, found that the response of directionally selective ganglion cells in the rabbit retina was essentially invariant over a wide range of contrasts. In addition, the low semisaturation constant of our effective contrast response function indicates a specialized sensitivity to low-contrast stimuli. It should be noted that primate lateral-geniculate-nucleus (LGN) cells appear to fall into two classes in terms of contrast sensitivity. Magnocellular LGN cells have contrast sensitivities in the range of human contrast sensitivity, which have thresholds in the neighborhood of 1% or less.[26] Parvocellular cells, on the other hand, have much lower contrast sensitivities, with corresponding thresholds around 10%, far above the psychophysical threshold. To the extent that our results show differences below 10% contrast and no differences in performance above this value, it would appear that our psychophysical findings are mediated by LGN magnocellular activity.

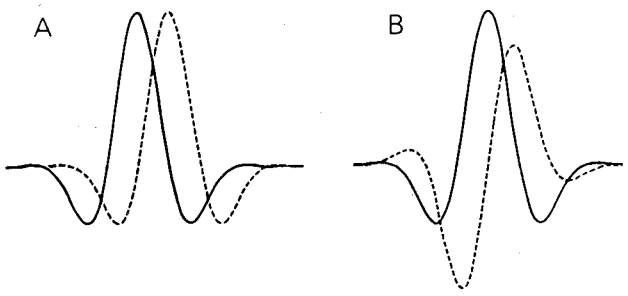

Fig. 10. Two configurations of RF's feeding a motion sensor that have been proposed by Van Santen and Sperling.[28] In A, two symmetric receptive fields are displaced. In B, the receptive fields are centered on the same region of space, one being spatially symmetric, the other being spatially antisymmetric.

Second, there is the spatial separation of RF's mediating directional selectivity in relation to their size. Two general schemes have been proposed, both of which require spatial separation of receptive fields differing by a spatial phase angle of 90° at their preferred spatial frequency. In a first case, the receptive-field centers of symmetric RF's are offset (Fig. 10A). In a second case, a symmetric and an antisymmetric receptive field is centered on the same retinal locus (Fig. 10B). It should be noted that both schemes have been outlined by Van Santen and Sperling.[27] The symmetric–antisymmetric scheme has been emphasized especially by Watson and Ahumada[28] based on theoretical research by Marcelja[29] and on electrophysiological results by Pollen and Ronner.[30]

Do our results fit into this general scheme? They fit most closely if we just think of those receptive fields having a center frequency that is identical to the sinusoidal-grating frequency. Here, the 90-deg phase shift is optimal for discrimination, and, assuming linearity, a contrast-sensitivity function proportional to sine (θ) would be expected. What about the complication introduced by the existence of mechanisms tuned to higher and lower spatial frequency with concommitant optimal phase predictions that are greater or less than 90°? Although these off-frequency mechanisms will receive less than optimal stimulation, they could influence contrast sensitivity. This would depend on a number of additional factors, including the relative contrast sensitivity of each mechanism, the physiological interaction between mechanisms, and the probability summation. To the extent that off-frequency receptive fields contribute significantly to thresholds, they would tend to broaden the contrast-sensitivity-versus-phase-angle function. As such, it is possible that the $\sin(\theta)$ relation described in Fig. 5 is a smeared composite of more sharply tuned phase functions for individual motion-detecting elements.

Relation to Experiments Using Random Dots: Are We Studying the Short-Range Process?

We introduced this paper by referring to experiments in which motion sensitivity was isolated by the use of random-dot

stimuli. The advantage of random dots is that we can be sure that we are isolating a motion system. They have the disadvantage of being spectrally broad, however, and cannot isolate mechanisms sensitive to different ranges of spatial frequency, especially in comparison with experiments using sinusoidal gratings. We suggest that our experiments with gratings are isolating the same short-range motion system as revealed by the random dots. We support this by noting that the dichoptic stepping of a sinusoidal grating by the optimum spatial phase of 90° does not lead to a motion percept,[31] a result that is consistent with a corresponding lack of motion seen in random dots under a similar dichoptic presentation.[1]

The results of Green and Blake[31] also imply that the upper displacement limit seen in random dots is spatial-frequency dependent rather than merely distance dependent. In the original experiments, Braddick[1] found a limit of 15 arc min, which in our case corresponds to spatial frequency of 2 cyc/deg, assuming that 180° is just beyond the limit where motion can be encoded. Green and Blake[31] found a clear motion percept with the 90° displacement of much lower spatial-frequency gratings, which suggests that the spatial limit for the short-range motion process is a peculiarity associated with the high-spatial-frequency information contained in random-dot stimuli. In particular, it has been found that D_{max} increases when a random-dot pattern is blurred or when larger pixels are used.[4,5]

Relation to Motion Hyperacuity Thresholds

In this paper we have developed a set of hypotheses relating contrast sensitivity, displacement thresholds, and effective contrast. Because this theoretical approach outlines how the minimum displacement threshold for motion is determined (see Fig. 7), it provides by definition an outline about how motion hyperacuity is determined. The basic idea is that motion hyperacuity is limited by signal-to-noise ratios of detectors having band-limited receptive fields spaced at optimal intervals. This means that several parameters in addition to RF size, including contrast sensitivity and the effective contrast response function, must be evaluated before we can make an estimate of the hyperacuity threshold.

In the case of the human observer, the high contrast sensitivity to see motion in sinusoidal gratings might lead one to predict a low displacement threshold or hyperacuity limit when the grating contrast is increased to 100%. In particular, linear theory, as embodied in Eq. (4), would predict a motion-hyperacuity threshold of 1 arc sec or less. That this is not the case suggests that contrast saturation poses a significant limitation in the encoding of small displacements and thus largely determines the motion-hyperacuity threshold.

APPENDIX A: DETECTION SENSITIVITY AS A FUNCTION OF PHASE ANGLE

Detection sensitivity is assumed to be proportional to distance in phasor space (see text). Referring to Fig. 2A:

$$|\mathbf{S}| = (\Delta X^2 + \Delta Y^2)^{0.5}, \tag{A1}$$

$$\mathbf{S}^2 = \Delta X^2 + \Delta Y^2, \tag{A2}$$

$$\mathbf{S}^2 = (A - A\cos\theta)^2 + (-A\sin\theta)^2, \tag{A3}$$

where A is the amplitude of the vector and θ is the angle jumped:

$$\mathbf{S}^2 = 2A^2(1 - \cos\theta), \tag{A4}$$

$$|\mathbf{S}| = 2A\left[\frac{(1 - \cos\theta)}{2}\right]^{1/2}, \tag{A5}$$

$$|\mathbf{S}| = 2A\sin(\theta/2). \tag{A6}$$

ACKNOWLEDGMENTS

Research for this paper was supported in part by grants 5P30 EY-01186, 1R01 EY-03884, and 1R01 EY-05408 from the National Institutes of Health and the Smith-Kettlewell Eye Research Foundation.

We would like to thank J. Nachmias and J. P. Thomas for comments on an earlier version of the manuscript.

REFERENCES

1. O. Braddick, "A short-range process in apparent motion," Vision Res. **14,** 519–527 (1974).
2. C. L. Baker and O. J. Braddick, "The basis of area and dot number effects in random dot motion perception," Vision Res. **22,** 1253–1260 (1982).
3. C. L. Baker and O. J. Braddick, "Does segregation of differently moving areas depend on relative or absolute displacement?" Vision Res. **22,** 851–856 (1982).
4. K. Nakayama and G. H. Silverman, "Temporal and spatial properties of the upper displacement limit in random dots," Vision Res. **24,** 293–299 (1984).
5. J. J. Chang and B. Julesz, "Displacement limits for spatial frequency filtered random-dot cinematograms in apparent motion," Vision Res. **23,** 1379–1385 (1983).
6. J. S. Lappin and H. H. Bell, "The detection of coherence in moving random-dot patterns," Vision Res. **16,** 161–168 (1976).
7. D. C. Burr and J. Ross, "Contrast sensitivity at high velocities," Vision Res. **22,** 479–484 (1982).
8. A. J. Pantle, "Temporal frequency response characteristics of motion channels measured with three different psychophysical techniques," Percept. Psychophys. **24,** 285–294 (1978).
9. S. P. McKee, D. Y. Teller, and S. Klein, "Statistical properties of forced-choice psychometric function: implication for probit analysis," Percept. Psychophys. (to be published).
10. We note some fundamental differences between our comparison of detection and discrimination thresholds and two other studies that might be construed as similar: A. B. Watson, P. G. Thompson, B. G. Murphy, and J. Nachmias, "Summation and discrimination of gratings moving in opposite directions," Vision Res. **20,** 341–348 (1980); M. Green, "Contrast detection and direction discrimination of drifting gratings," Vision Res. **23,** 281–289 (1983)]. These studies used drifting gratings rather than stepped gratings. Most important was the difference in task, requiring the observer to detect the presence or absence of a grating rather than the presence or absence of a displacement. Thus the intent and the interpretation of the detection versus the discrimination in these studies are not directly applicable to the experiments reported here.
11. C. Blakemore and F. W. Campbell, "On the existence of neurons in the human visual system selectively sensitive to the orientation and size of retinal images," J. Physiol. **203,** 237–260 (1967).
12. I. Ohzawa, G. Schlar, and R. E. Freeman, "Contrast gain control in the cat visual cortex," Nature **298,** 266–268 (1982).
13. K. Nakayama, "Differential motion hyperacuity under conditions of common image motion," Vision Res. **21,** 1475–1482 (1981).
14. K. Nakayama and C. W. Tyler, "Psychophysical isolation of motion sensitivity by removal of familiar position cues," Vision Res. **21,** 427–433 (1981).
15. G. Westheimer, "Spatial phase sensitivity for sinusoidal grating targets," Vision Res. **18,** 1073–1074 (1978).
16. D. G. Watt and M. Morgan, "The recognition and representation

of edge blur; evidence for spatial primitives in human vision," Vision Res. **23,** 1465–1477 (1983).
17. R. Sekuler, A. Pantle, and E. Levinson, "Physiological basis of motion perception," in *Handbook of Sensory Physiology*, R. Held, H. Liebowitz, and H. Terler, eds. (Springer-Verlag, New York, 1978), Vol. III, pp. 67–96.
18. M. Keck, F. W. Montague, and T. P. Burke, "Influence of the spatial periodicity of moving gratings on motion response," Invest. Ophthalmol. Vis. Sci. **19,** 1364–1370 (1980).
19. M. Keck, T. D. Palella, and A. Pantle, "Motion aftereffect as a function of the contrast of sinusoidal gratings," Vision Res. **16,** 187 (1976).
20. G. Legge, "A power law for contrast discrimination," Vision Res. **21,** 457 (1981).
21. D. Albrecht and D. B. Hamilton, "Striate cortex of monkey and cat: contrast response function," J. Neurophysiol. **48,** 217–237 (1982).
22. K. Nakayama, "Local adaptation in LGN neurons: evidence for a surround antagonism," Vision Res. **11,** 501–509 (1971).
23. H. B. Barlow and W. R. Levick, "Three factors affecting the reliable detection of light by ganglion cells of the cat," J. Physiol. (London) **200,** 1–24 (1969).
24. D. J. Tolhurst, J. A. Movshon, and A. F. Dean, "The statistical reliability of signals in single neurons in cat and monkey visual cortex," Vision Res. **23,** 775–785 (1983).
25. H. B. Barlow and R. M. Hill, "Selective sensitivity to direction of motion in ganglion cells in the rabbit's retina," Science **139,** 412–414 (1963).
26. E. Kaplan and R. M. Shapley, "*X* and *Y* cells in the lateral geniculate nucleus of macaque monkeys," J. Physiol. **330,** 125–143 (1982).
27. J. P. H. Van Santen and G. Sperling, "A temporal covariance model of human motion perception," J. Opt. Soc. Am. A **2,** 300–321 (1985).
28. A. B. Watson and A. J. Ahumada, "A look at motion in the frequency domain," NASA Tech. Memo. 84352 (1983).
29. S. Marcelja, "Mathematical description of the responses of simple cortical cells," J. Opt. Soc. Am. **70,** 1297–1300 (1980).
30. D. A. Pollen and S. F. Ronner, "Phase relationship between adjacent single cells in the visual cortex," Science **22,** 1409–1411 (1981).
31. M. Green and R. Blake, "Phase effects in monoptic and dichoptic temporal integration: flicker and motion detection," Vision Res. **21,** 365–372 (1981).